Full length article

Direct ageing experiments on nanometre-scale aluminium alloy samples

J. Banhart [a,b,1,*], Y.-S. Chen [a], Q.N. Guo [b], R.K.W. Marceau [c], J.M. Cairney [a]

[a] *Australian Centre for Microscopy and Microanalysis, The University of Sydney, NSW 2006, Australia*
[b] *Helmholtz Zentrum Berlin for Materials and Energy, Hahn-Meitner-Platz 1, 14109 Berlin, Germany*
[c] *Deakin University, Institute for Frontier Materials, Geelong, Victoria 3216, Australia*

ARTICLE INFO

ABSTRACT

Studies of the kinetics of precipitation in aluminium alloys help to understand the role of quenched-in excess vacancies in the ageing process. Investigations of ageing in nanometre-sized samples are valuable because excess vacancies are believed to anneal out quickly while the alloy is still supersaturated with solute atoms. We prepare samples suitable for atom probe tomography (APT) with a sharp tip of some tens of nm radius and verify that they can be solutionised and quenched, after which they are still suitable for APT. The investigated Al-Zn alloy is known to show extremely strong clustering after quenching of the bulk material but we find that this clustering is completely suppressed in solutionised and quenched samples. Precipitation calculations explain this by a fast loss of vacancies, within seconds, during and after quenching. As such calculations also suggest that at elevated temperatures clustering could occur in the thermal equilibrium, we carry out exploratory ageing experiments on APT samples at 100°C and 135°C. No clusters are found in such samples, which could be related to experimental restrictions (Zn losses) or unfavourable nucleation conditions in nm-sized samples.

1. Introduction

Vacancies play a crucial role in determining the kinetics of precipitation in aluminium alloys. After solutionising and quenching, excess vacancies are retained in the lattice and accelerate ageing at low temperatures (e.g. at 'room temperature') by many orders of magnitude. Only after such excess vacancies have annealed out, is the equilibrium precipitation rate reached, which at ∼20°C is very low. During ageing at various temperatures, the progress of precipitation is jointly controlled by the rate of vacancy annihilation and the temperature dependence of the diffusion parameters of the solutes involved, but their influence is hard to separate due to the lack of reliable experimental data. Positron annihilation spectroscopy provides some insight into vacancy dynamics but as positrons are sensitive to both vacancies and emerging atomic clusters and precipitates, a precise determination of the vacancy fraction during quenching and ageing is normally not possible. Recent modelling efforts have shown how the two factors influence precipitation, for example during constant heating rate

experiments [1]. A recent novel experiment has provided insights through ageing of nm-sized samples and measurement of atomic arrangements by atom probe tomography (APT) [2]. Due to the small dimensions of the samples involved, excess vacancies anneal out within seconds during and after quenching without causing much precipitation while solute supersaturation is still high. In an Al-Mg-Si alloy, natural ageing (NA in short in the following) was found to be suppressed for 3 weeks due to the lack of excess vacancies [2].

Here, experiments similar to the ones in Ref. [2] are carried out with another alloy, namely Al-10 wt.%Zn (4.38 at.%) instead of Al-Mg-Si. Al-Zn shows a much stronger tendency for clustering at 'room temperature' than any Al-Mg-Si alloy. Electrical resistivity increases – attributed to clustering – by a few percent in just a few minutes in Al-Zn alloys, whereas in Al-Mg-Si alloys the increase occurs over a period of weeks after solutionising and quenching. NA in Al-Mg-Si creates very small clusters that even by APT analysis are hard to identify [3], whereas in Al-Zn, clusters are a few nanometres in diameter already after hours of NA and contain hundreds of Zn atoms, which makes these clusters very easy to identify even by visual inspection of reconstructed APT data [4].

Another advantage of studying Al-Zn alloys is that they can be solutionised at much lower temperatures than other alloys. For around 5 at.% Zn, the solvus temperature is 190°C to 200°C

---

* Corresponding author.
E-mail address: banhart@helmholtz-berlin.de (J. Banhart).
[1] Temporary affiliation: Australian Centre for Microscopy and Microanalysis, The University of Sydney, NSW 2006, Australia.

[5] compared to more than 500°C for most Al-Mg-Si alloys. This might enable one to apply direct ageing to APT samples – even in air without too much oxidation – and to avoid the two-stage procedure described in Ref. [2] that involves solutionising samples of typically 25 μm thickness and then electropolishing them to nm thickness at −40°C. A key to success is the moderate vapour pressure at lower solutionising temperatures that might not give rise to excessive Zn losses. In Al-Mg-Si alloys, loss of Mg during solutionising of small samples is a concern and has been experimentally shown [2]. Another objective of the present work is to check whether APT samples that have been solutionised and quenched – so that they no longer contain excess vacancies – can be aged under equilibrium conditions at temperatures high enough to provide enough thermal vacancies and solute diffusion.

Here, we first verify that APT samples can be solutionised (by 'nano-solutionising'), quenched and then successfully analysed by APT. It is shown that clustering during NA is suppressed. Application of a model verifies that this is due to excess vacancy annihilation. In a further exploratory step, we try to stimulate precipitation in nano-solutionised and quenched atom probe samples by ageing at elevated temperatures, which the model calculations suggest to be possible from the viewpoint of sufficient solute diffusion.

2. Experimental

A Al-Zn alloy was prepared by melting 90 wt.% Al (purity 99.95%) and 10 wt.% Zn (= 4.38 at.%) (purity 99.995%) in a crucible, stirring mechanically and decanting the melt into a rectangular mould. The resulting block was then homogenised at 480°C for 24 h in an argon atmosphere and cut into pieces with surfaces removed. The pieces were cold-rolled to 1 mm thickness and cut into strips of 1 mm × 4 mm cross-section. These strips were thereafter cold extruded to 1 mm diameter, annealed at 220°C for 1 h in an argon atmosphere and then slowly cooled to 'room temperature' in the furnace. Wire drawing to 0.49 mm diameter provided material for further studies. Such wires are very convenient both for electrical resistivity measurements and as starting materials for the preparation of APT samples. Additionally, the texture of the drawn wire specimens is consistent and therefore also the grain orientation of the atom probe samples, such that apparent density differences of Zn due to crystallographically influenced field-induced effects (refer to details in Sec. 3 and Fig. 3) are also consistent between samples, effectively normalising the issue for quantitative comparison between samples. Material from two wires was used for APT (called no. 1 and 2).

About 3-cm long pieces of alloy wire were fixed in a small steel wire frame to facilitate handling and inserted into a pre-heated alumina crucible for solutionising. After a given time, the entire frame was dropped into ice water. NA at 20°C was conducted for 1 h to 8 days. Some samples were aged at 100°C or 135°C in an oil bath. APT samples were prepared from these samples as well as from untreated wires.

Pieces of Al-Zn wire were first electrolytically rough-polished in perchloric acid (concentration 25%) applying the double-layer method [6] until necking approximately in the middle of the sample occurred, after which each of the then tapered half-samples was further electrolytically fine-polished in perchloric acid (concentration 2%) using a micro loop [6] to obtain the final sample with a tip sharp enough for APT. The samples were crimped inside copper tubes to provide mechanical support and electrical conduction in the APT.

Solutionising and quenching of APT samples was conducted in an air circulation furnace at various temperatures between 255°C and 350°C for various times. We shall call this procedure 'nano solutionising' to distinguish it from conventional 'bulk solutionising' of macroscopic samples. To protect the APT samples, they were mounted in a protective sleeve in which the crimped copper tube holding the APT needle was fixed by a screw, see Fig. 1. A hole in the sleeve allows the quenching medium (ice water) to come in contact with the sharp tip of the aluminium alloy specimen. Some of the samples were allowed to age at 20°C for 45 min to 24 h after quenching. Others were artificially aged at 100°C or 135°C in an oil bath, in which case the APT samples together with the sleeve were slid into a Pyrex test tube that was then evacuated and sealed. In some cases, the state of the APT samples was checked by SEM for bending, fracture, etc., before conducting APT experiments. However, when time was a limiting factor, samples were directly analysed by APT without prior checking.

A CAMECA Local Electrode Atom Probe (LEAP) 4000X Si was employed for atom probe measurements (except for one sample where a LEAP 3000 Si was used). Measurements were conducted at 50 K with electric pulses repeated at a rate of 200 kHz and a pulse fraction of 20%. In most cases, field evaporation started after the voltage had reached 2.5 to 5 kV.

Reconstruction and analysis of APT data were carried out with software IVAS 3.6. Mass spectra contained peaks of hydrogen, aluminium and zinc, see supplementary Fig. S2. The built-in modules 'nearest neighbour distribution' and 'cluster analysis' were used. Table 1 lists the experiments relevant for this study and specifies the concentration of Zn in the APT samples as calculated from the numbers of different atom species detected in the data sets.

The evolution of electrical resistivity after quenching was measured in-situ at 20 ± 0.1°C in an oil bath on coiled wires of ~400 mm length and 0.82 mm diameter using a four-point probe and an electric current of 100 mA.

3. Results and discussion

3.1. Bulk solutionising and natural ageing

The electrical resistivity increases directly after solutionising (at 260°C) and quenching, as Fig. 2a shows. Maximum resistivity is reached after just 17.5 minutes, after which resistivity decreases again. After 1 day, the changes in resistivity become very small. Such behaviour is well documented in the literature [7] and reflects fast clustering at 20°C, which increases resistivity, and ensuing coalescence and growth of clusters that lead to a reduction of resistivity. The solutionising temperature strongly influences the kinetics of NA: After solutionising at 300°C, for example, the maximum resistivity is reached after just 4.5 min. The kinetics are governed by an Arrhenius law with an activation energy of 0.75 eV ±0.06 eV (inset of Fig. 2a) in accordance with the value of 0.7 eV given in Ref. [7]. This activation energy is close to that of vacancy formation in Al (0.67±0.03 eV [8]) and therefore the change of kinetics can largely be attributed to the fraction of excess vacancies at the solutionising temperature. Structurally, the decomposition of the supersaturated solid solution in Al-Zn for the present composition is coherent below 100°C to 120°C [9] (or even higher [10]) and involves the formation of initially small spherical clusters that later become oblate ellipsoids with a rhombohedrally distorted crystal structure [5].

Atom probe tomography measurements were conducted on a series of samples cut from wire 2, bulk-solutionised at 300°C for 30 min, quenched in ice water and then naturally aged. Clustering is already clearly visible in the unsegmented atom probe data. Application of the maximum separation method [6,11] allows identification of the clusters and to quantify the fraction of Zn atoms bound in clusters and the concentration of Zn remaining in the matrix. The former quantity varies from very small to 42% in the 11 data sets obtained in a series in which NA time varied between 1 h and 6 h. Correspondingly, the residual matrix concentration of Zn drops. Fig. 2b shows an example of a segmented data set.
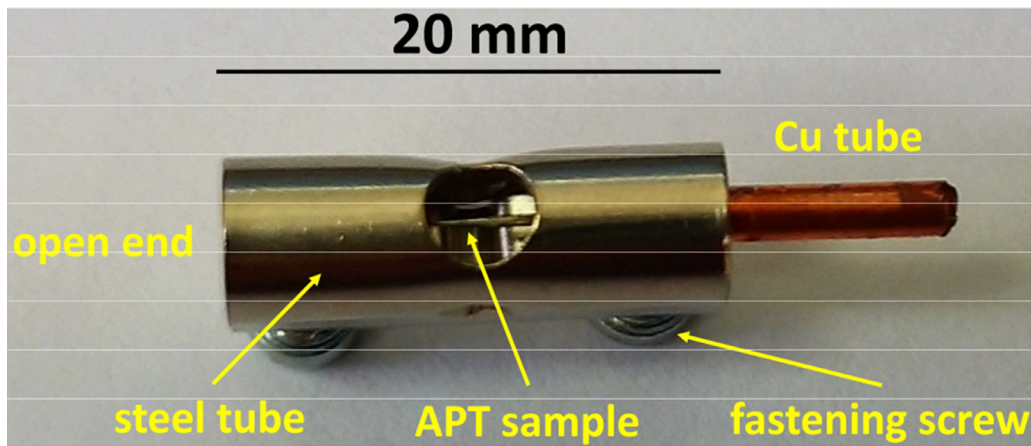
Fig. 1. Steel holder for atom probe samples. The sample is held by a screw fixing the crimped copper tube and the tip of the sample is visible in the centre hole. This holder was used to protect samples both during solutionising and quenching, allowing the quenching medium (cold water) to reach it, and for the ageing treatments at 100°C and 135°C in an oil bath.

Table 1
Zn content in various specimens calculated from the number of detected Zn atoms related to the total number of detected Al and Zn atoms in various APT data sets. Nominal Zn content in samples is 4.38 at.%.

Wire no.	Solutionsing (T, t)	Ageing (T, t)	No. samples	Zn content from APT (at.%)	Data shown in Fig.
bulk solutionising					
1	255°C, 15 min	20°C, 4.5^h – 8^d	14	3.56 ± 0.52	
1	350°C, 15 min	20°C, 66^h	6	3.92 ± 0.50	
2	300°C, 30 min	20°C, 1^h – 6^h	9 (11 measurements[3])	4.19 ± 0.19	2b, 2c
2	350°C, 120 min	100°C, 4^h – 24^h	5	3.91 ± 0.44	4, 9c
nano solutionising					
1	255°C, 15 min	20°C, 45^m – 1^d	3 (5 measurements[2])	3.74 ± 0.60	3, 5, 6, 7
1	350°C, 8 min	20°C, 1^h	2	3.42 ± 0.13	
2	300°C, 15 min	100°C, 4^d/6^d	3 (4 measurements[3])	2.27 ± 0.25	9a,b
2	350°C, 120 min	100°C, 82^d	1[1]	0.94	
2	350°C, 10 min	135°C, 82^d	2	2.53 ± 0.28	

[1] measured on LEAP 3000.
[2] including re-polished samples.
[3] one sample re-started in a second APT run.

No monotonic relationship between ageing time and the Zn fraction in clusters or matrix composition was found, as seen in Fig. 2c, where the progress of clustering is not directly related to NA time. Such a relationship was given for nominally the same alloy and solutionising temperature (for 1 h) in Ref. [4], where the Zn concentration in the matrix was reported to drop continuously from 3.4 to 1.4 at.% (0.69 to 0.29 relative to nominal composition) for NA times from 2.5 h to 12 h, respectively (but only for 3 samples). These concentrations are slightly lower than the present ones.

Average cluster diameters are in the range (1.5–3.5) nm in the samples (largest clusters 10 nm) with number densities in the range (0.3–3) × 10^{24} m^{-3}. The Zn concentration in the cluster varies only weakly around 42±3 at.%.

A possible explanation for the unclear relationship between ageing time and extent of clustering could be a varying Zn content between the various samples. A higher local Zn content would accelerate clustering. However, the Zn content given for each sample in Fig. 2c (open squares) does not confirm this. For example, one sample aged for 2 h and showing strong clustering (encircled triangle) has a lower Zn concentration that the two samples NA for 5 h that show little clustering.

Another possibility is, that precipitation might not have been completely uniform in our Al-Zn alloy, so that the small region imaged by APT was not always representative. This interpretation is supported by the results of another series of naturally aged samples based on wire 1 and 15 min of solutionising at 255°C (Table 1, first line). In that series we found an even more pronounced

non-uniformity of clustering and in some cases, no clustering was observed for a NA time that produced clusters in other samples, although the Zn content found in the respective volumes was very similar. It has been reported in the literature that Zn clusters in Al-3 at.% Zn alloys are 'arranged in nests', with cluster-free areas of 30 nm diameter, after solutionising at 400°C and NA for 17 days [12]. The origin of such non-uniformities was not discussed and is still not entirely clear.

Two different wires were used in these experiments. A possibility that the Zn content in the two samples might have been different was not confirmed by the analysis of Zn concentrations calculated from APT data sets, see Table 1. Although the concentration for wire 2 might appear slightly higher (3rd line in Table 1), the values for wire 1 are still within the margin of experimental scatter. All values are slightly lower than the nominal value corresponding to the 10 wt.% Zn contained in the cast alloy.

We find, empirically, that at a solutionising temperature of 300°C no more cluster-free samples are encountered when NA times exceed 2 h, Fig. 2c. Combined with the findings reported in Ref. [4], the experiments confirm previous reports that in Al-Zn alloys of the composition chosen here, NA leads to very pronounced clustering for more than 2 h NA time and that saturation of NA is reached quickly, probably after 12 h.

3.2. Nano-solutionising and natural ageing

Electropolished APT samples were directly nano-solutionised and quenched. The solutionising temperature was chosen between
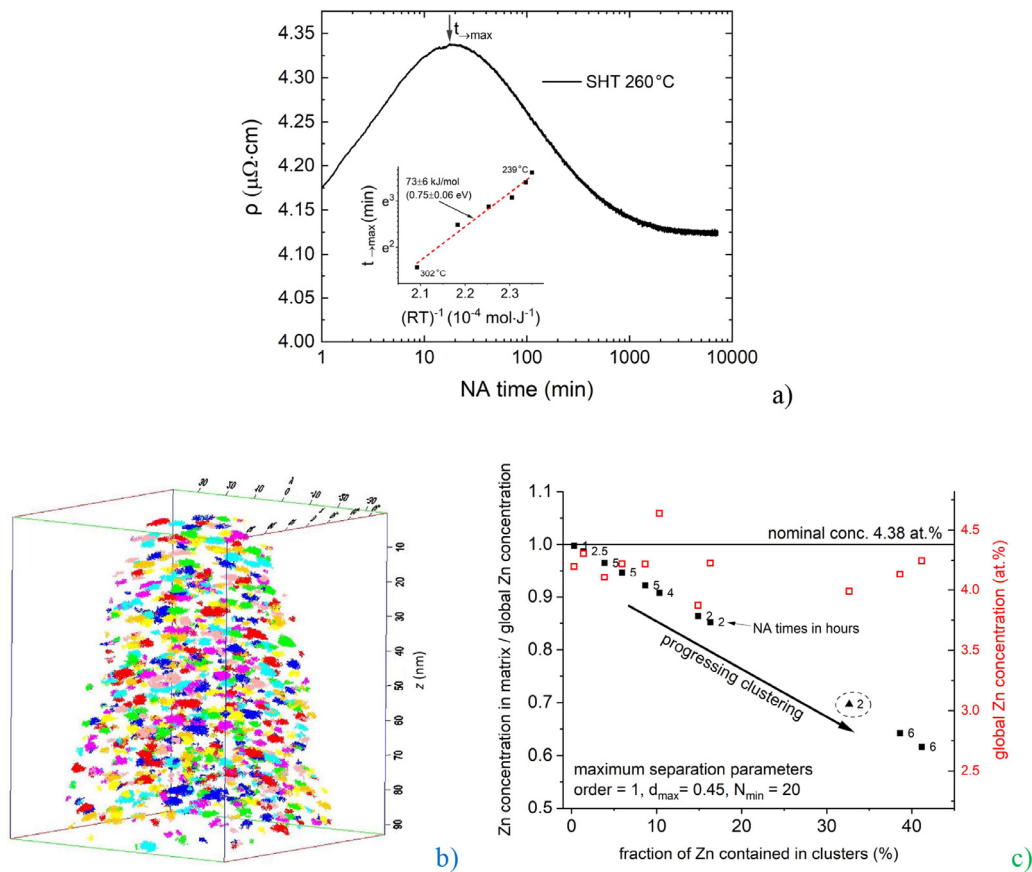
Fig. 2. a) Electrical resistivity of Al-Zn alloy measured at 20°C during natural ageing (NA) directly after solutionising (260°C for 30 min) and quenching. The inset features an Arrhenius analysis of the time needed to reach maximum resistivity for different solutionising temperatures. b) APT reconstruction of alloy bulk-solutionised at 300°C for 30 min, ice water quenched and naturally aged for 2 h (encircled triangle in Fig. 2c). Box size is $78 \times 78 \times 92$ nm^3 (x,y,z). The maximum separation cluster search algorithm (d_{max}=0.45, N_{min}=20) was applied to segment the 1028 clusters displayed in different colours here. c) Cluster properties of samples solutionised at 300°C for 30 min and naturally aged for the times given in the graph. Solid symbols: residual Zn concentration in the matrix relative to the measured total concentration (given by open symbols) as a function of the fraction of all Zn atoms contained in one of the clusters.

255°C and 350°C for 8 to 15 min and was conducted in air. These parameters were selected considering that the vapour pressure of Zn should be sufficiently low to avoid excessive Zn losses. According to published values for the vapour pressure, we obtain 0.02 Pa for 255°C (see Fig. S1). The Zn concentration measured in five nano-solutionised, quenched and NA samples was found to be close to that in the bulk aged samples, see Table 1, lines 5 and 6. Therefore, Zn losses are indeed small in this case.

Solutionising has to lead to a uniformly supersaturated solute solution and thermal vacancies must be created at the surface of an APT sample and diffuse into the sample. The rate limiting process is diffusion of Zn in the Al matrix that is slower than diffusion of vacancies. From the diffusion parameters of Zn given in the caption of Fig. 8, a diffusion coefficient for Zn in Al at 255°C of 6×10^{-17} m^{2}s^{-1} is obtained. Correspondingly, a Zn atom needs 7 s to travel 50 nm at 255°C, the approximate radius of an APT sample, see e.g. Fig. 4. As vacancies diffuse faster than Zn atoms, they reach the interior of the sample in a shorter time. The solutionising times chosen are therefore sufficiently long.

Five APT samples were 'successfully' processed, i.e. yielded a minimum of 2.5×10^6 atoms. The success rate was just below 50% because another 6 samples failed early. None of the data sets show visible clusters in the 3D visualisation (not shown) after up to 24 h of NA. Based on the discussion in Ref. [2], this was expected because of vacancy annihilation during solutionising and quenching. In Sec. 3.3 this will be assessed quantitatively. In the following the

absence of clusters will be verified more rigorously than by visual inspection.

Most of the reconstructed atom probe datasets exhibit a varying density of Al and Zn atoms. The Al density is lower around the poles of the fcc lattice and the density of Zn atoms is higher along lines radiating from the poles of the fcc lattice. Such density differences are related to the crystallography of the specimen tip and are known to occur due to electrostatic field enhancement at atomic terraces [6], particularly for low-order crystallographic poles with greater lattice spacing and lead to trajectory aberration, for the Al atoms in this case, and field-induced migration of the Zn atoms [13]. Fig. 3 provides views along the needle axis of a 30-nm thick slice and shows the density fluctuations of both Al and Zn.

Two of the 5 samples that did not fracture during APT measurement were electrolytically re-polished to create new APT samples by removing a few 100 µm of the sample from its tip and preparing a new APT sample from a volume more deeply embedded in the former bulk material, as schematically explained in Fig. 4. One such re-polished sample was successfully analysed and showed pronounced clustering, therefore resembling the bulk-solutionised samples in Sec. 3.1 (further discussion below). At 500 µm distance from the original tip, the thickness of the needle is 60 µm assuming a shank angle of 7° estimated from Fig. 4 (left). Therefore, the material in this area resembles the bulk and the diffusion time of vacancies to the surface is about 10^6 times higher than in the tip, where the thickness is about 10^3 times smaller, see further comments in Sec. 3.3.
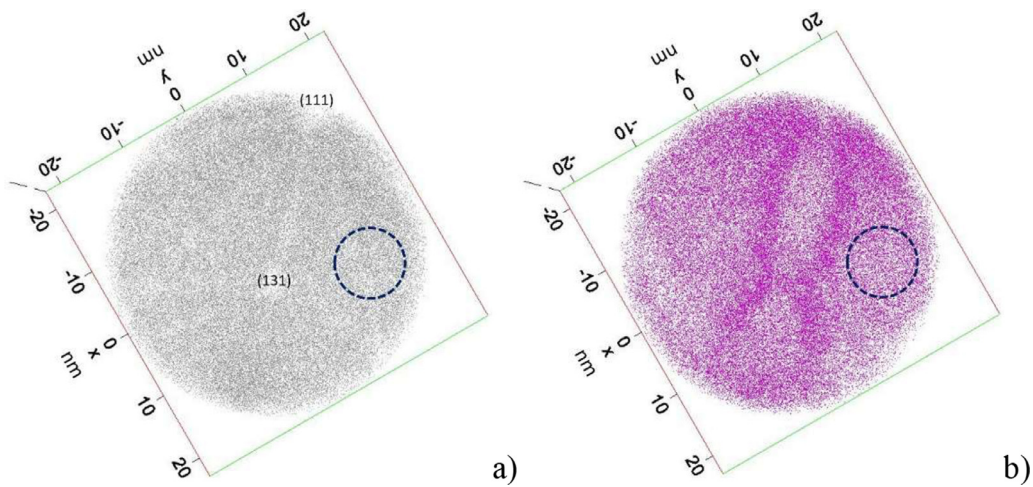
Fig. 3. Reconstruction of a) Al and b) Zn atom positions in a sample nano-solutionised at 255°C for 15 min, quenched and naturally aged for 4 h. The circle defines a long cylinder along the needle axis (z) – centre coordinates (8,12,z) – in which the atomic density appears nearly constant.
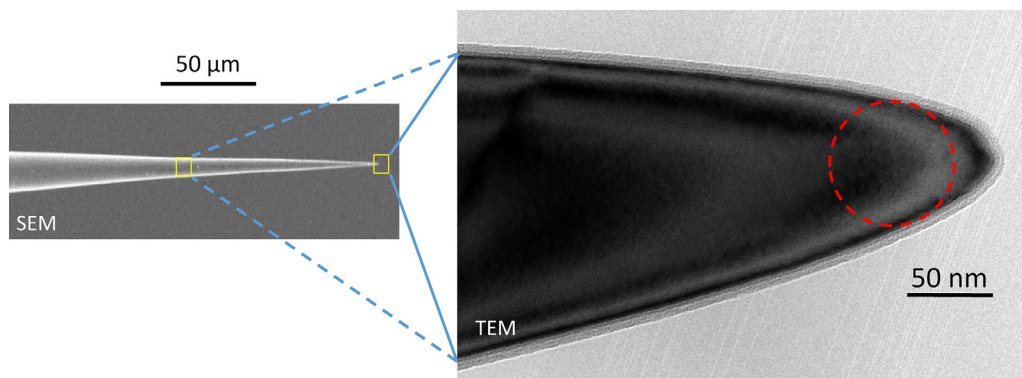

Fig. 4. Low-magnification SEM (taken with a JEOL Neoscope Tabletop SEM) and higher-magnification TEM (taken with a JEOL 2200FS) images of an APT sample (bulk-solutionised and aged at 100°C for 4h). Such SEM images were used to check the integrity of APT tips. This image also illustrates the principle of re-polishing of APT samples: After evaporating the original tip (right yellow box) the sample was electrolytically back-polished to create a new tip (left yellow box). A few APT samples were transferred to the TEM to assess their shape and the oxide layers formed. Here, a ~8 nm thick oxide layer is seen. The broken red circle marks a sphere of 30 nm radius and indicates that the tip is sharp enough for APT.

In order to verify that the samples are free of clusters we apply two types of analyses. The analysis software IVAS 3.6 provides the distribution of nearest neighbours, which can be used as an indicator for clustering if compared to randomised data sets. It has been argued that the choice of the fifth nearest neighbour distribution (5NN) provides a sensitive quantity for detecting minute traces of clusters as formed during NA in Al-Mg-Si alloys, where clusters are by far smaller than in Al-Zn alloys [14,15]. Fig. 5 shows such 5NN distributions of Zn atoms for the five nano-solutionised and naturally aged samples and also the re-polished sample exhibiting visible clusters. The former show distributions (black) very similar to randomised distributions (red). In the latter sample, smaller distances are much more frequent in the measured data set than in the randomised one.

Three of the samples show a small difference between the measured and randomised data in that that the measured data exhibits a slightly lower and broader peak shifted to slightly smaller 5NN distances. The deviation is smaller than that detected in Ref. [14] and interpreted as a sign of NA there, but it could point to a small signature of cluster formation.

Therefore, as a second indicator, the radial distribution function (RDF) of Zn atoms was calculated following a suggestion in Ref. [2]. Its calculation involves counting the number N_{Zn} of Zn atoms in a shell of radius R and width ΔR around a selected Zn atom, repeating this for all Zn atoms in a given volume, and summing the

numbers to obtain a histogram $\bar{N}_{Zn}(R, \Delta R)$. The same procedure is applied to a randomised data set $N_{Zn}^{rnd}(R, \Delta R)$. In order to reduce statistical fluctuations especially for small R, where $N_{Zn}(R, \Delta R)$ is small, the randomization is carried out 100 times, thus reducing randomization noise by a factor of 10. Finally, the ratio between the randomised and the non-randomised data set is calculated, and *relative radial distribution functions (RDFs)* $f_{Zn}(R, \Delta R)$ are obtained. Further details of the randomization procedure are described in the Online Supplement S3. It deviates from the procedure given in Ref. [2] in some details. The resulting RDFs corresponding to the frequency histograms in Fig. 5 are shown in Fig. 6.

The suspicion that the distribution is not perfectly random in three of the samples is confirmed by the relative RDFs of the 5 samples in question, see Fig. 6b, since perfect randomness of the Zn distribution would imply $f \equiv 1$. The error bars confirm that at least two of the samples show a small but notable tendency of Zn correlation for distances up to some nanometres, while the 3 others – and especially the sample NA for 24 h – show less or little sign of clustering. Still, the signal describing the two former samples featuring a maximum f-value below 1.1 is very small compared to that of the re-polished sample exhibiting clearly visible clusters and f-values up to 4.5, see Fig. 6a. Ref. [2] has reported f-values up to 1.2 even in random samples and explained this by effects such as density fluctuations in the sample, more specifically migration of Si to the poles in the evaporation field (in Al-Mg-Si
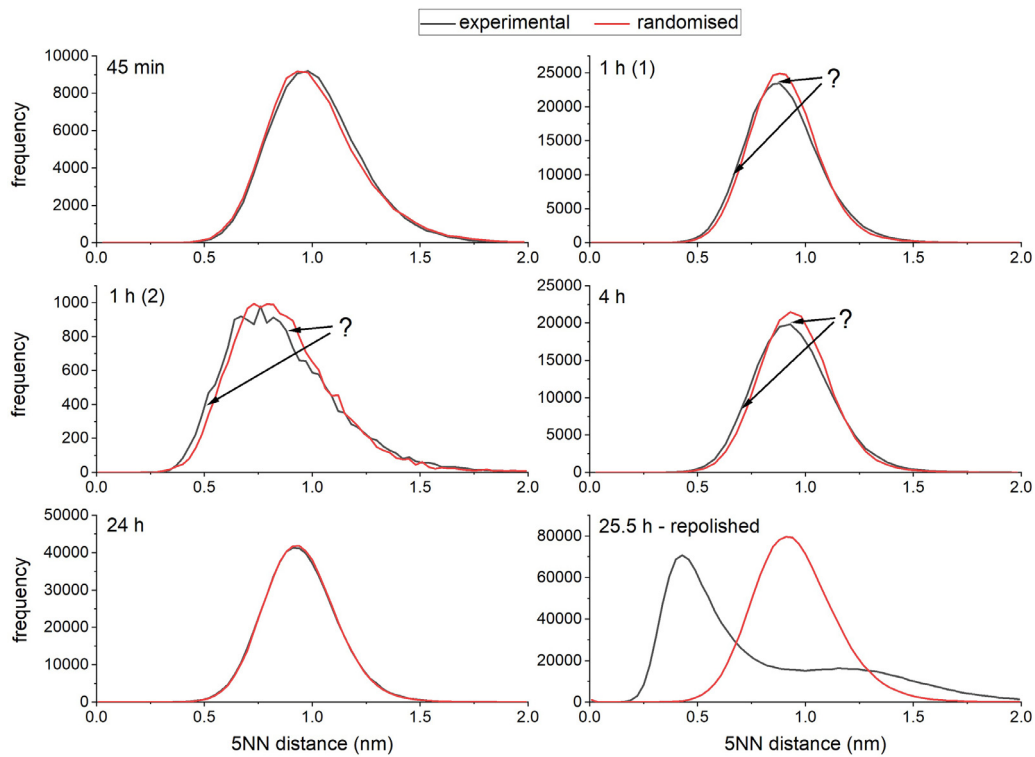
Fig. 5. Frequency histograms (black: experimental; red: randomised) of 5NN distances between Zn atoms in APT samples nano-solutionised at 255°C for 15 min, water-quenched and naturally aged for the times specified. The sample on the lower right is the one NA for 24 h, but re-polished after APT measurement and measured again after in total 25.5 h of NA. Arrows mark positions at which slight deviations from randomness could be suspected. The sample aged for 1 h (2) shows pronounced noise due to low statistics.
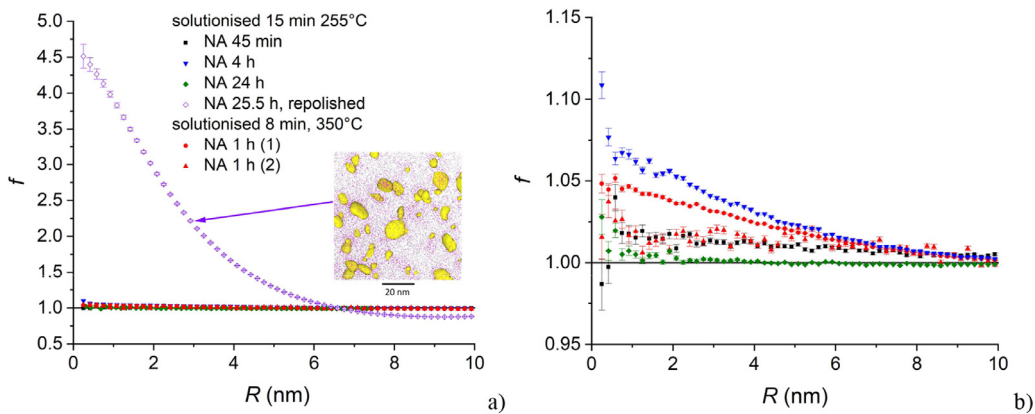
Fig. 6. Relative radial distribution functions $f_{Zn}(R, \Delta R)$ (ΔR=0.25 nm) of the samples discussed in Fig. 5. a) Data for the re-polished sample shows a pronounced variation that is related to strong clustering, see also inset featuring 18% Zn iso-surfaces. b) Magnification of the f-axis and data from the five nano-solutionised samples (same legend as in a)).

alloy). In the case discussed here, the slight signature for Zn clustering could be caused by Zn density elevations in certain regions of the sample. As mentioned above, such regions can be already visually discerned in reconstructions as areas of increased Zn density radiating from poles, Fig. 3b.

To demonstrate this we calculate $f_{Zn}(R, \Delta R)$ for the sample NA for 4 h separately for Zn atoms inside one of 15 spheres of radius 10 nm, see Fig. 7a. Their average (orange broken line) is identical to the uppermost curve in Fig. 6b. The various curves differ significantly and in some spheres clustering is less pronounced than in others. Variations occur mainly when moving perpendicular to the axis of the APT sample (=z direction), as seen when looking at groups of 3 spheres displaced by the z-coordinate only. The corresponding curves are close together. In view of the heterogeneities

visible in most of the samples (especially clear in the 4 h NA sample, Fig. 3b) the suspicion that local Zn gradients create the false impression of clustering seems justified.

In order to further verify this interpretation, it was attempted to restrict data to a slim cylinder parallel to the APT sample axis in which the atomic density appears uniform by visual inspection. After several trials a cylinder was found that gives rise to the RDF in Fig. 7b. Despite some fluctuations for small radii this relative RDF suggests a random distribution of Zn. To summarise this section, clustering in nano-solutionised Al-Zn alloy is indeed suppressed in analogy to the report in Ref. [2] for Al-Mg-Si alloys.

The $f_{Zn}(R, \Delta R)$ found for the re-polished sample do not differ from such functions obtained for samples just bulk solutionised and NA in the traditional manner except for the magnitude of f
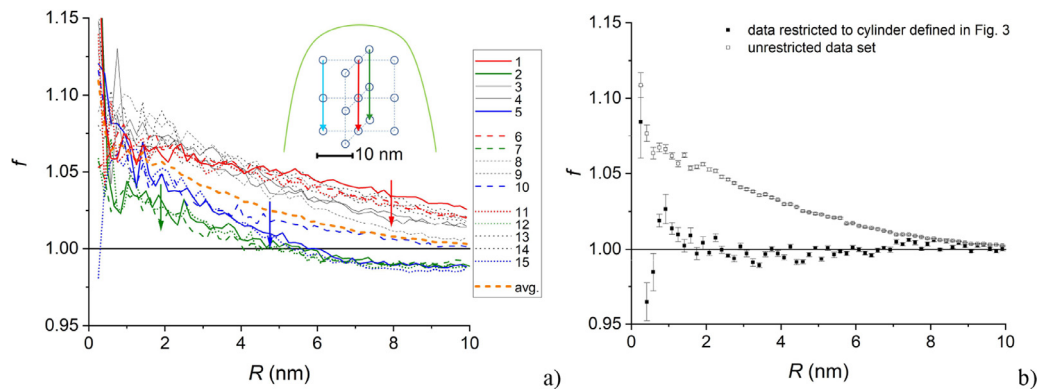
Fig. 7. a) Relative RDFs calculated separately for Zn atoms in one of 15 spheres of radius 10 nm for the nano-solutionised sample NA for 4 h. Orange broken line is average of all. The drawing in the inset shows how the 15 spheres (only centres shown as blue circles) are oriented in the APT sample (green contour). The coloured arrows mark sequences of 3 volumes along a path parallel to the sample axis. b) Relative RDF calculated in a slim cylinder parallel to the axis of the APT sample as defined in Fig. 3.

and the radius at which f reaches a value of 1, see supplementary Sec. S5.

3.3. Calculations

The formation and growth of clusters can be described mechanistically as the diffusion-driven migration of solute atoms with the help of an attached vacancy. Solute-vacancy complexes eventually collide with other solute atoms or already formed solute clusters. During such encounters solute–solute or solute–cluster complexes are formed. In most cases, the vacancy detaches from such complexes and assists the diffusion of other solute atoms. The mechanism of repeated vacancy-solute attachment and detachment has been termed the "vacancy-pump" model [16]. Only very simple models exist to describe such phenomena [17,18]. An additional complication is that the vacancy site fraction is not constant whenever non-equilibrium states such as after quenching are involved. A very large excess of vacancies with respect to the thermal equilibrium may exist for a limited time and only after the annihilation of all the excess vacancies at grain boundaries or dislocation jogs an equilibrium is reached.

A recently developed formalism combines a model of vacancy diffusion and annihilation with a model of solute diffusion and clustering [1]. Vacancy dynamics are given by Ref. [19], while solute diffusion is treated using solute diffusion parameters taken from ab-initio calculations [20]. The process of clustering is simplified by assuming a constant success rate of solute attachment to solutes or existing clusters, which is independent of all other parameters. This approach neglects nucleation barriers and effects of cluster dissolution. Despite the simplicity of the assumption involved the kinetics of clustering in Al-Mg-Si alloy was described very well [1]. For this reason we employ the model here.

Fig. 8b shows the progress of clustering in 3 different cases as calculated applying the model of Ref. [1] and using reasonable parameters for Zn diffusion. The alloy with 50 μm grain radius, bulk aged at 260°C, quenched and then NA at 20°C shows two-step ageing (blue lines). The first step is due to quenched-in excess vacancies and is completed in 12 h after reaching ~40% of the total clustering potential, i.e. when 40% of all Zn atoms have been transported to clusters. This value has been taken from APT results (highest value in Fig. 2c) and the correspondence was achieved by setting the abovementioned success rate of solute attachment to 10^{-3}. This is the only adjustable parameter and implies that in 1 out of 1000 cases of an encounter between a diffusing Zn atom and another solute or an already existing cluster the Zn atoms remains permanently attached. This value is 10 times higher than the one used to model Al-Mg-Si alloys and expresses the much faster clus-

tering rate in Al-Zn alloy. After about 5 d, all the excess vacancies have annihilated (Fig. 8a) and clustering progresses at a very low rate. After 3 years (10^8 s), slight further clustering is noted and completion of clustering requires about 1000 years under equilibrium conditions at 20°C.

If the grain radius is reduced to 50 nm – a typical dimension of an atom probe sample, see Fig. 4 – the scenario changes completely (red lines): During quenching and in the first few seconds at 20°C, the excess vacancies already anneal out through the surface of the APT sample (Fig. 8a), and consequently ageing progresses only slowly (Fig. 8b). In fact, at 20°C it requires 3 years at equilibrium vacancy concentration to lead to a first visible increase of the volume fraction α of clusters. As such conditions are not user friendly in experiments, an increase of temperature is considered. Ageing an APT sample at 100°C after nano-solutionising and quenching (green lines) also eliminates all excess vacancies within fractions of a second (Fig. 8a), but accelerated diffusion at 100°C could lead to notable clustering after a few hours (Fig. 8b).

As pointed out above, by re-polishing previously nanosolutionised and NA samples we place a part of a sample into the APT tip that was in an about 60-μm thick volume before re-polishing. Such a thick volume can be compared to the grains in the bulk-aged samples, i.e. fast cluster formation is observed.

The calculations presented here provide necessary conditions for clustering, namely that atoms can be transported to clusters in a given time. They are not sufficient since no information on the solubility of solute atoms nor on possible nucleation barriers is included. Real precipitation times could therefore be longer. In the next section, some trial experiments attempting to verify equilibrium vacancy ageing in an APT sample at elevated temperatures are presented.

3.4. Trial experiments on nano-solutionising and ageing at elevated temperatures

APT samples were aged in an oil bath, either at 100°C or 135°C, for ageing times between 1 h and 82 days, after nano-solutionising and quenching. The choice of these temperatures was motivated by literature studies in which a high number density of precipitates was obtained for ageing temperatures between 80°C and 133°C [21] and by our calculations that suggest that sufficient ageing within a few hours would be supported by sufficient solute diffusion. The coherent solvus temperature for the investigated alloy is 120°C [5], so coherent precipitation could theoretically occur at 100°C, although it is not clear whether this can be expected in nm-sized samples. At 135°C, incoherent precipitation should occur.
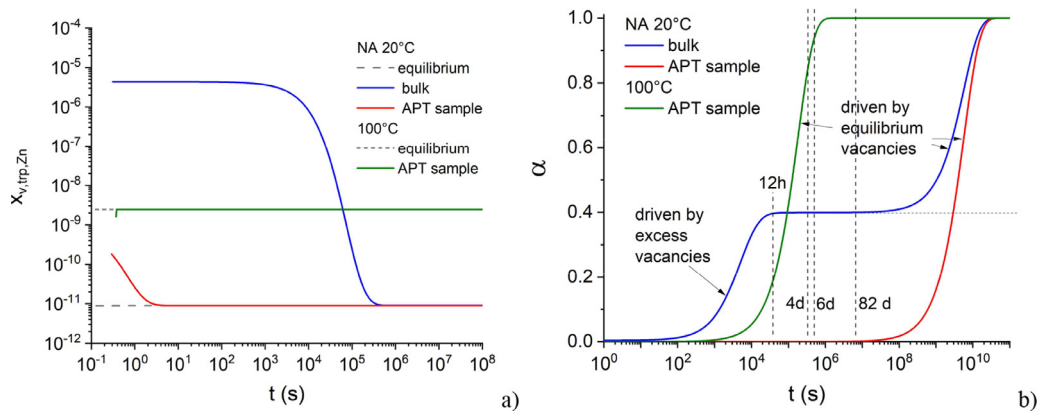
Fig. 8. Calculated vacancy and cluster properties in Al-Zn alloy (4.38 at.%Zn) after solutionising at 260°C and quenching. a) Site fraction of vacancies trapped at Zn sites, b) Volume fraction α of Zn clusters. Blue lines: bulk sample (grain radius 50 μm, dislocation density 4×10^{11} m^{-2}, jog spacing 0.02 atom^{-1}) during NA. Red lines: APT sample ('grain' radius 50 nm, dislocation-free), during NA. Green lines: APT sample during ageing at 100°C. Some of the experimental ageing times applied at 100°C are given as vertical broken lines. The formalism and parameters described in Ref. [1] were used. The specific parameters for Zn atoms were 0.05 eV for Zn-V binding [22] and the Zn diffusion pre-factor $D_0 = 2.7 \times 10^{-5}$ m^{2}s^{-1} and activation energy $Q = 1.22$ eV (average from two almost identical data sets [23,24]).
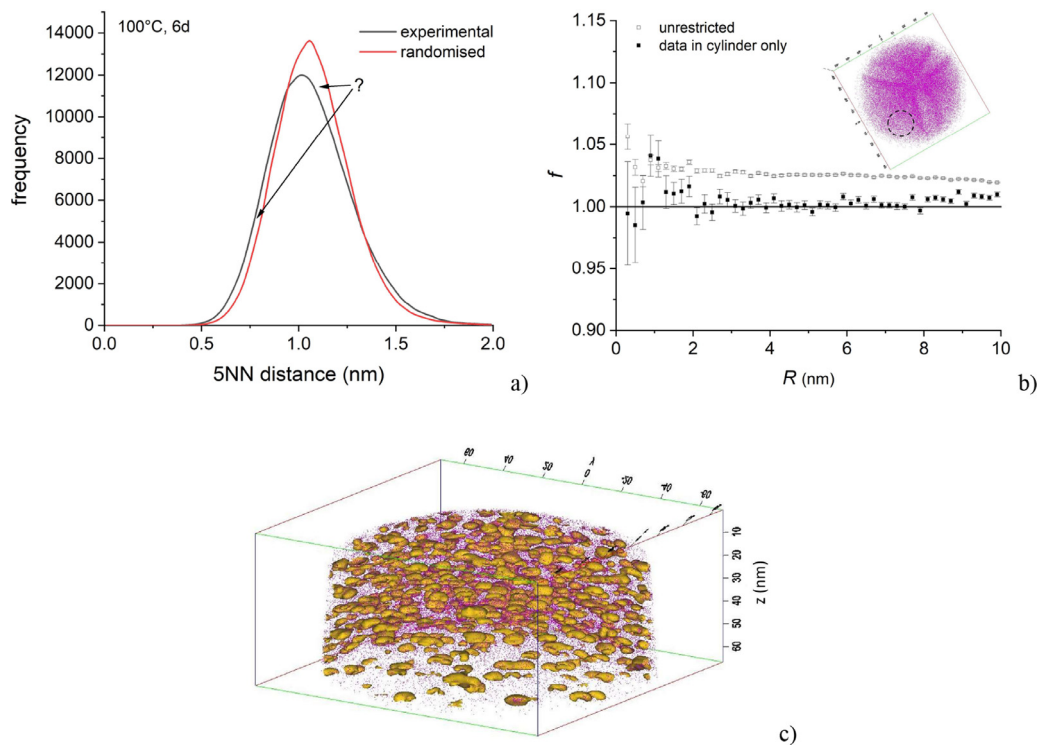

Fig. 9. a) Frequency histogram (black: experimental; red: randomised) of 5NN distance between Zn atoms in a sample nano-solutionised (300°C, 15 min), quenched and aged at 100°C for 6 days. b) Relative RDFs calculated for the same sample. The open symbols refer to all Zn atoms in 7 spheres of 10 nm radius distributed evenly over the entire volume, full symbols describe only Zn atoms inside a slim cylinder marked by a dotted circle in the inset that extends along the needle axis. This cylinder is outside areas of varying Zn densities. c) Sample bulk-solutionised (350°C, 2h) and quenched, then aged at 100°C for 4 h. Strong clustering is observed, visualised here by 10% Zn isosurfaces (in orange). Purple dots are Zn atoms in the matrix. Box size is $135 \times 140 \times 64$ nm^3 (x,y,z).

APT experiments on aged samples yielded mixed results. From a total of 22 samples, 10 failed directly, while 4 yielded only little data (<2.5 million atoms). Failure was especially pronounced for samples aged for 82 days, where only 3 of 13 samples yielded good data. Surprisingly, 2 samples that had been accidentally exposed to oil due to fracture of the protective test tube yielded around 3 million atoms. The Zn content of all the samples was found to be lower than in the samples that were only nano-solutionised and NA and, especially, one sample aged for 80 days contained only 0.94 at.% Zn, see Table 1. This sample had been nano-solutionised at 350°C for 2 h, which most likely is the reason for such large Zn losses. Artificial ageing both at 100°C and 135°C seems to reduce

the Zn content, as can be seen by comparing lines 2 and 9, and also lines 3 and 7, of Table 1.

None of the reconstructed data showed visible clustering of the type observed for bulk-annealed samples or incoherent precipitation of Zn. Heterogeneities occurred that were similar to the ones in the naturally aged samples, see inset in Fig. 9b. The 5NN frequency histograms exhibit a slight deviation from a random distribution (Fig. 9a), which could be taken as a sign of slight clustering. Correspondingly, the relative RDF also exhibits slight Zn-Zn correlation vs. the random configuration as f reaches values up to 1.05 (Fig. 9b, open symbols). Similar to the discussion in Sec. 3.2, this effect disappears if analyses are restricted to volumes of more uni-

form Zn distribution, for example to the slim cylinder marked by a dotted circle in Fig. 9b. The atoms in such a volume have relative RDFs very close to 1 (Fig. 9b, full symbols).

All the other samples aged at 100°C and 135°C for up to 82 days show similar frequency histograms and relative RDFs as the one described in Fig. 9 and therefore clustering cannot be confirmed for any of these samples.

In order to demonstrate that clustering is actually expected for the ageing temperatures chosen in our alloy, a set of ageing experiments at 100°C and 135°C was carried out on bulk-solutionised and quenched samples. Fig. 9c shows the strong clustering obtained after 4 h of ageing at 100°C.

The absence of precipitation in these experiments could have various explanations: i) The conditions for nucleation are not as favourable in nanometer-sized samples as in bulk samples, noting that the model applied in Sec. 3.3 does not take account of nucleation barriers that might exist in APT samples due to the absence of nucleation points (e.g. dislocations). (ii) The Zn content in the samples has dropped to a level that is too low (basically to ∼60% of the original values, see Table 1) so that the driving force for precipitation is no longer strong enough at the temperatures applied. After a reduction of Zn content to 2.2 at.%, the solvus temperature would have dropped to 110°C. For 2.5 at.%, it would be very close to 135°C [9]. This implies that ageing at 100°C would lead to precipitation, but possibly not ageing at 135°C.

3.5. Outlook

Future experiments might benefit from in-situ heating devices, which allow one to flash-heat atom probe samples in ultra-high vacuum near the measurement position. In such measurements, the solutionising times and temperatures could be further reduced and the negative influence of the ambient conditions occurring in ex-situ experiments (oxidation and fracture of APT samples) avoided.

Using alloys higher in zinc would compensate Zn losses, increase the driving force for clustering, more likely allow for coherent precipitation, and increase the number density of clusters. Possibly, precipitation under equilibrium conditions would be observable in such alloys. Mapping the ageing temperature/time regime more completely, e.g. applying temperatures notably above 20°C but below 100°C, might also increase the chance for finding clustering under equilibrium conditions.

4. Conclusions

- Al-Zn alloy atom probe samples prepared by electropolishing can be solutionised at up to 350°C in air and quenched, after which 50% of them still can be run in the atom probe in the voltage-pulse mode. Loss of zinc is observed but remains at acceptable levels.
- Natural ageing in nano-solutionised samples is effectively suppressed. The reason is the loss of excess vacancies in accordance with calculations and with the literature. This happens despite the much higher driving force for clustering in Al-Zn alloys compared to the previously investigated Al-Mg-Si alloys.
- Ageing at elevated temperatures after nano-solutionising could lead to cluster formation according to calculations, but the trial experiments carried out do not provide evidence for this. Possibilities for future improved experiments are discussed.

Declaration of competing interest

The authors declare that they have no known competing financial interests or personal relationships that could have appeared to influence the work reported in this paper.

Supplementary materials

Supplementary material associated with this article can be found, in the online version, at doi:10.1016/j.actamat.2022.117848.

References

[1] Z. Yang, J. Banhart, Natural and artificial ageing in aluminium alloys - the role of excess vacancies, Acta Mater 215 (2021) 117014.
[2] P. Dumitraschkewitz, P.J. Uggowitzer, S.S.A. Gerstl, J.F. Löffler, S. Pogatscher, Size-dependent diffusion controls natural aging in aluminium alloys, Nat. Commun. 10 (2019) 4746.
[3] F. De Geuser, B. Gault, Metrology of small particles and solute clusters by atom probe tomography, Acta Mater 188 (2020) 406–415.
[4] Y. Komiya, S. Hirosawa, T. Sato, 3DAP Analysis and computer simulation of nanocluster formation in the initial aging stage of Al-Zn alloys, Mater. Sci. Forum 519-521 (2006) 437–442.
[5] H. Löffler, Structure and Structure Development of Al-Zn alloys, Akademie Verlag, Berlin, 1995.
[6] B. Gault, M.P. Moody, J.M. Cairney, S.P. Ringer, Atom Probe Microscopy, Springer, New York, 2012.
[7] C. Panseri, T. Federighi, A Resistometric Study of Pre-Precipitation in Al-10-Percent Zn, Acta Metall. Mater. 8 (1960) 217–238.
[8] P. Ehrhart, Atomic Defects in Metals - Al, in: H. Ullmaier (Ed.), Landolt-Börnstein - Group III Condensed Matter 25, Springer Verlag, Berlin, Heidelberg, 1991.
[9] J.L. Murray, The aluminium-zinc system, Bull. Alloy Phase Diagr. 4 (1983) 55–73.
[10] H. Löffler, C. Eschrich, O. Simmich, Recalculation of several metastable phase lines of the Al-Zn system, phys. stat. sol. (a) 113 (1989) 269–275.
[11] D.J. Larson, T.J. Prosa, R.M. Ulfig, B.P. Geiser, T.F. Kelly, Local Electrode Atom Probe Tomography - A User's Guide, Springer, New York, 2013.
[12] R. Ramlau, H. Löffler, Guinier-Preston Zones in an A1-3 at% Zn Alloy, phys. stat. sol. (a) 68 (1981) 531.
[13] B. Gault, F. Danoix, K. Hoummada, D. Mangelinck, H. Leitner, Impact of directional walk on atom probe microanalysis, Ultmi 113 (2012) 182–191.
[14] R.K.W. Marceau, A. de Vaucorbeil, G. Sha, S.P. Ringer, W.J. Poole, Analysis of strengthening in AA6111 during the early stages of aging: atom probe tomography and yield stress modelling, Acta Mater 61 (2013) 7285–7303.
[15] R.K.W. Marceau, Atomic-scale analysis of light alloys using atom probe tomography, Mater. Sci. Technol. 32 (2016) 209–219.
[16] I.A. Girifalco, H. Herman, A model for growth of Guinier-Preston zones - the vacancy pump, Acta Metall. Mater. 13 (1965) 583–590.
[17] H.S. Zurob, H. Seyedrezai, A model for the growth of solute clusters based on vacancy trapping, Scripta Mater 61 (2009) 141–144.
[18] M. Madanat, M. Liu, J. Banhart, Reversion of natural ageing in Al-Mg-Si alloys, Acta Mater 159 (2018) 163–172.
[19] F.D. Fischer, J. Svoboda, F. Appel, E. Kozeschnik, Modeling of excess vacancy annihilation at different types of sinks, Acta Mater 59 (2011) 3463–3472.
[20] M. Mantina, Y. Wang, L.Q. Chen, Z.K. Liu, C. Wolverton, First principles impurity diffusion coefficients, Acta Mater 57 (2009) 4102–4108.
[21] G. Laslaz, P. Guyot, Etude par microscopie electronique de la decomposition de l'alliage Al-6.8 at.% Zn, Acta Metall. Mater. 25 (1977) 277–285.
[22] J. Peng, S. Bahl, A. Shyam, J.A. Haynes, D.W. Shin, Solute-vacancy clustering in aluminum, Acta Mater 196 (2020) 747–758.
[23] D. Beke, I. Godeny, F.J. Kedves, G. Groma, Diffusion of Zn-65 in dilute AlZn, AlMg, AlZnMg and AlZnFe alloys, Acta Metall. Mater. 25 (1977) 539.
[24] A.W. Nicholls, I.P. Jones, Determination of low-temperature volume diffusion-coefficients in an Al-Zn alloy, J. Phys. Chem. Solids 44 (1983) 671–676.